4

Lepton flavor violation and leptogenesis in A_4 based discrete flavor symmetric radiative seesaw model

We have studied the radiative seesaw model also known as scotogenic model proposed by Ernest Ma, which is an extension of the Standard Model by three singlet right handed neutrinos and a scalar doublet. This model proposes that the light neutrinos acquire a non-zero mass at 1-loop level. In this work, realisation of the scotogenic model is done by using discrete symmetries $A_4 \times Z_4$ in which the non-zero θ_{13} is produced by assuming a non-degeneracy in the loop factor. Considering different lepton flavor violating(LFV) proceses such as $l_\alpha \longrightarrow l_\beta \gamma$ and $l_\alpha \longrightarrow 3l_\beta$, their impact on neutrino phenomenology is studied. We have also analysed $0\nu\beta\beta$ and baryon asymmetry of the Universe(BAU) in this chapter.

4.1 Introduction:

Standard model(SM) has been the most successful model of particle physics which is supported by a large amount of experimental evidences. But, SM fails to provide proper explaination for some imporant problems of modern physics, such as absolute neutrino mass [178], baryon asymmetry of universe(BAU) [179, 180], dark matter [181, 182] etc. The quest for these unexplained physical problems results in the several SM extensions, aiming at a common explanation for these issues. The scotogenic model proposed by Ernest Ma [73] is one such attractive framework where SM is minimally extended. In this framework, SM is extended by a scalar doublet and three singlet fermions which are charged under Z_2 symmetry. This inbuilt discrete symmetry forbids the usual tree level generation of neutrino mass. Neutrino mass is generated at 1-loop level within this model. Phenomenology of scotogenic model has been adressed in various literatures [183, 110, 184, 185].

The scotogenic model is probably the simplest TeV scale model that can simultaneously account for neutrino masses and dark matter. In this model, lepton flavor violating processes, such as $\mu \to e\gamma$ and $\mu \to 3e$, also takes place at 1-loop, via diagrams analogous to those responsible for neutrino masses. Lepton flavor violation(LFV) in the scotogenic model has already been studied[186, 187]. However, most of the literature primariliy foucses on $\mu \to e\gamma$ due to its stringent experimental limit whereas other decays are rarely considered. Here, in this work, we have LFV in details along with other phenomenologies. We know that the baryon asymmetry of universe is one the most important problems which cannot be adressed in SM as it fails to satisfy the Sakharov conditions [109], which demands baryon number (B) violation, C and CP violation, and departure from thermal equilibrium. We are therefore, intersested to study BAU in the framework of scotogenic model. We can incorporate baryogenesis via leptogenesis [179], where a net leptonic asymmetry is generated first, which further gets converted into baryogenesis through $(B+L)$ violating electroweak sphaleron phase transitions [188]. As discussed in many literatures [189, 190], it is known

that there exists a lower bound of about 10TeV for the lightest of the right handed neutrino in the Scotogenic model considering the vanilla leptogenesis scenario [180, 110]. Thus, in our work, a similar kind of leptogenesis takes place. One of the most important significance of BSM frameworks is to study the origin of neutrino mass along with charge lepton mixing and identifying possible symmetries related to this. By incorporating symmetries to a model one can make a model more general and predictive as it will corelate two or more free parameters of the model or make them vanish. Discerete flavor symmetric realisation of sctogenic model is done in a very few work [191, 192].

In this work we realised the scotogenic model through $A_4 \times Z_4$ discrete flavor symmetry. The implications of the discrete symmetry can be seen as it contraints the Yukawa couplings of a particular model. Here, we produce a realistic neutrino mixing to do an extensive analysis of lepton flavor violating processes. Considering different lepton flavor violating(LFV) proceses such as $l_\alpha \to l_\beta \gamma$ and $l_\alpha \to 3l_\beta$, we analysed their impact on the neutrino phenomenology as well. The most stringent bounds on LFV comes from the MEG experiment [41]. The limit on branching ratio for the decay of $\mu \to e\gamma$ from this experiment is obtained to be $\text{Br}(\mu \to e\gamma) < 4.2 \times 10^{-13}$. In case of $l_\alpha \to 3l_\beta$ decay contraints comes from SINDRUM experiment [42] is set to be $\text{BR}(\text{l}_\alpha \to 3\text{l}_\beta) < 10^{-12}$. Neutrinoless double beta decay($0\nu\beta\beta$) is also studied within the model by the consideration of the constraints from KamLAND-Zen experiment. We have also incorporated BAU within the model and have shown the viable parameter space satisfying the Planck bound.

The rest of the chapter is organized as follows: in section(4.2) we introduce the model whereas in section(4.3) we realise the scotogenic model using $A_4 \times Z_4$ symmetry. Section(4.4) and (4.5) contains the discussions on LFV processes and leptogenesis respectively. Phenomenological analysis of the model is given in section(4.6).

4.2 Radiative seesaw Model

Radiative seesaw model is an extension of the IHDM [76, 193–196] and the IHDM is nothing but a minimal extension of the SM by a Higgs field which is a doublet under $SU(2)_L$ gauge symmetry with hypercharge $Y = 1$ and a built-in discrete Z_2 symmetry [73–77]. The necessity of this modification took place as the inert Higgs doublet model(IHDM) could only accommodate dark matter, whereas it failed in explaining the origin of neutrino masses at a renormalizable level . In this model, three neutral singlet fermions N_i with $i = 1,2,3$ are added in order to generate neutrino masses and assign them with a discrete Z_2 symmetry. Here, N_i is odd under Z_2 symmetry, whereas the SM fields remain Z_2 even. Symbolic transformation of the particles under Z_2 symmetry is given by,

$$N_i \longrightarrow -N_i,\ \eta \longrightarrow -\eta,\ \phi \longrightarrow \phi,\ \Psi \longrightarrow \Psi, \tag{4.1}$$

where η is the inert Higgs doublet, ϕ is the SM Higgs doublet and Ψ denotes the SM fermions. The new leptonic and scalar particle content can thereafter be represented as follows under the group of symmetries $SU(2) \times U(1)_Y \times Z_2$:

$$\begin{pmatrix} \nu_\alpha \\ l_\alpha \end{pmatrix}_L \sim (2, -\frac{1}{2}, +),\ l^c_\alpha \sim (1,1,+),\ \begin{pmatrix} \phi^+ \\ \phi^0 \end{pmatrix} \sim (2, \frac{1}{2}, +),$$

$$N_i \sim (1,1,-),\ \begin{pmatrix} \eta^+ \\ \eta^0 \end{pmatrix} \sim (2, 1/2, -). \tag{4.2}$$

The scalar doublets are written as follows :

$$\eta = \begin{pmatrix} \eta^\pm \\ \frac{1}{\sqrt{2}}(\eta^0_R + i\eta^0_I) \end{pmatrix}, \quad \phi = \begin{pmatrix} \phi^+ \\ \frac{1}{\sqrt{2}}(h + i\xi) \end{pmatrix}. \tag{4.3}$$

We have no Dirac mass term with ν and N_i, however, the similar Yukawa-like coupling involving η is allowed. Nevertheless, the scalar cannot get a VEV. The neutrino mass can be

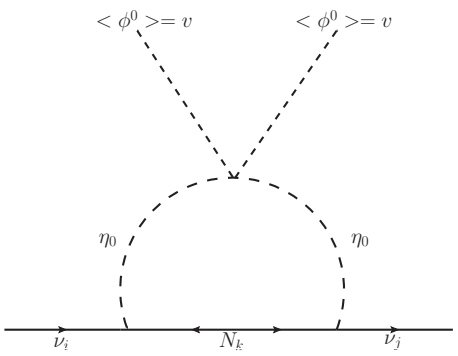

Fig. 4.1 One- loop contribution of neutrino mass generation with the exchange of right handed neutrino N_i and the scalar η_0.

generated through a one-loop mechanism, which is based on the exchange of η particle and a heavy neutrino. In figure, we see two Higgs fields ϕ^0 are involved. They will not propagate but will acquire VEV after the EWSB. The lagrangian involving the newly added field is :

$$\mathcal{L} \supset \frac{1}{2}(M_N)_{ij}N_iN_j + Y_{ij}\bar{L}\tilde{\eta}N_j + h.c \tag{4.4}$$

where, the 1^{st} term is the Majorana mass term for the neutrino singlet and the 2^{nd} term is the Yukawa interactions of the lepton. The new potential on addition of the new inert scalar doublet is:

$$\begin{aligned} V_{Scalar} =& m_1^2\phi^+\phi + m_2^2\eta^+\eta + \frac{1}{2}\lambda_1(\phi^+\phi)^2 + \frac{1}{2}\lambda_2(\eta^+\eta)^2 + \lambda_3(\phi^+\phi)(\eta^+\eta) \\ &+ \lambda_4(\phi^+\eta)(\eta^+\phi) + \frac{1}{2}\lambda_5[(\phi^+\eta)^2 + h.c.] \end{aligned} \tag{4.5}$$

All the parameters in Eq. (4.5) are real by hermicity of the Lagrangian, except for λ_5. Since, the bilinear term $(\phi^+\eta)$ is forbidden by the exact Z_2 symmetry, therefore one can always choose λ_5 real by rotating the relative phase between ϕ and η. Furthermore, after the spontaneous symmetry breaking like in the SM, we are left with one physical Higgs boson h which resembles the SM Higgs boson, as well as four dark scalars: one CP even(η_R^0), one CP

odd(η_I^0) and a pair of charged ones ($\eta^\pm$). The masses of these physical scalars are:

$$\begin{aligned} m_h^2 &= -m_1^2 = 2\lambda_1 v^2, \\ m_{\eta^\pm}^2 &= m_2^2 + \lambda_3 v^2, \\ m_{\eta_R^0}^2 &= m_2^2 + (\lambda_3 + \lambda_4 + \lambda_5) v^2, \\ m_{\eta_I^0}^2 &= m_2^2 + (\lambda_3 + \lambda_4 - \lambda_5) v^2. \end{aligned} \tag{4.6}$$

It is clear from the above equations that all the scalar couplings are written in terms of physical scalar masses and m_2 , thereby providing six independent parameters of the model to be : $\{m_2, m_h, m_{\eta_R^0}, m_{\eta_I^0}, m_{\eta^\pm}, \lambda_2\}$. Here, m_h is the mass of SM-Higgs, $m_{\eta_R^0}$, $m_{\eta_I^0}$ and $m_{\eta^\pm}$ are the masses of CP-even, CP-odd and charged scalars of the inert doublet respectively. In this work, as we have considered the CP-even scalar to be the lightest particle and a probable DM candidate, so we consider $\lambda_5 < 0$ without any loss of generality. Also, the limit $\lambda_5 \to 0$ leads to the mass degeneracy of the neutral components of the inert doublet. Following the 't Hooft scenario [197] , the smallness of λ_5 to obtain the lepton asymmetry, which would have been lost if considered to be zero, is acceptably natural. We have a simplified diagram shown in Fig. (4.2) that can be split further into two diagrams and from which the mass can be easily calculated by considering mechanism after EWSB.

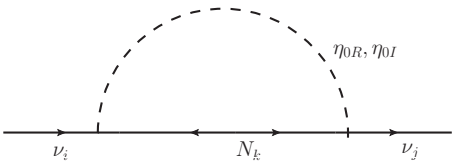

Fig. 4.2 One-loop diagram with exchange of η_R^0 and η_I^0. ν_i and ν_j representing two different generations of active neutrinos. N_i is the right handed neutrino.

Calculation on the basis of one diagram is sufficient and considered as other would be same except for η_R^0 replaced by η_I^0. The neutrino mass matrix arising from the radiative mass

model is given by :

$$\begin{aligned} M^{\nu}_{ij} &= \sum_k \frac{Y_{ik}Y_{jk}}{16\pi^2} M_{N_k} \left[\frac{m^2_{\eta^0_R}}{m^2_{\eta^0_R} - M^2_{N_k}} ln \frac{m^2_{\eta^0_R}}{M^2_{N_k}} - \frac{m^2_{\eta^0_I}}{m^2_{\eta^0_I} - M_{N_k}}^2 ln \frac{m^2_{\eta^0_I}}{M_{N_k}}^2 \right] \\ &\equiv \sum_k \frac{Y_{ik}Y_{jk}}{16\pi^2} M_{N_k} [L_k(m^2_{\eta^0_R}) - L_k(m^2_{\eta^0_I})], \end{aligned} \tag{4.7}$$

where M_k represents the mass eigenvalue of the mass eigenstate N_k of the neutral singlet fermion N_k in the internal line with indices j=1,2,3 running over the three neutrino generation with three copies of N_k and Y is the Yukawa coupling matrix. The function $L_k(m^2)$ used in Eq. (4.7) is given by:

$$L_k(m^2) = \frac{m^2}{m^2 - M^2_{N_k}} \ln \frac{m^2}{M^2_{N_k}} \tag{4.8}$$

4.3 Flavor Symmetric realization of radiative seesaw model:

In this section we have realised scotogenic model using $A_4 \times Z_4$ flavor symmetry. Scotogenic model already has an inbuilt Z_2 symmetry which provides the explanation of dark sector within this framework [73]. The particle content and respective charge corresponding to the discrete symmetries are given in Table 4.1. The discrete symmetries, i.e $A_4 \times Z_4$ will impose constraints on the Yukawa coupling matrix, thereby, constraining the model.

The Lagrangian for the charged lepton sector is given by:

$$\mathcal{L}_l = \frac{y_e}{\Lambda}(l_L \phi \chi_T) l^c_{R_1} + \frac{y_\mu}{\Lambda}(l_L \phi \chi_T) l^c_{R_2} + \frac{y_\tau}{\Lambda}(l_L \phi \chi_T) l^c_{R_3} \tag{4.9}$$

where, Λ is the cut-off scale of the theory and y_e,y_μ,y_τ are the coupling constants. Terms in the first parenthesis reperents the product of two triplets(l_L and χ_T) under A_4, each of these terms contracts with A_4 singlets 1,1$^{'}$ and 1$^{''}$ corresponding to l_{R1}, l_{R2} and l_{R3} respectively. When the flavon χ_T gets vaccum expectation value(vev), flavor symmetry will break and we will get the flavor structure for lepton. Finally it sets the charged lepton coupling matrix as

the diagonal one, once the flavon vev as well as Higgs vev are inserted. For the Dirac mass term, the effective Lagrangian can be written as:

$$\mathcal{L}_D = \frac{\eta}{\Lambda}[Y^{'} l_{L_i} N_i \chi_S + Y^{''} l_{L_i} N_i \chi]. \tag{4.10}$$

Again, the additional right handed neutral fermions are represented by the Lagrangian:

$$\mathcal{L}_{M_N} = M N_i N_j. \tag{4.11}$$

Now, let us consider the vev allignment of the flavons as follows[191]:

$< \chi_T >= v_T(1,0,0)$, $< \chi_S >= v_S(1,1,1)$, $< \chi >=$ u. With the above considerations, the charged leptonic mass matrix is given by:

$$M_l = \frac{v_T < \phi >}{\Lambda} \begin{pmatrix} y_e & 0 & 0 \\ 0 & y_\mu & 0 \\ 0 & 0 & y_\tau \end{pmatrix} \tag{4.12}$$

also, the Yukawa coupling matrix takes the form:

$$Y = \begin{pmatrix} 2a+b & -a & -a \\ -a & 2a & b-a \\ -a & b-a & 2a \end{pmatrix} \tag{4.13}$$

where, $a = Y^{'} \frac{v_S}{\Lambda}$ and $b = Y^{''} \frac{u}{\Lambda}$. From Eq.4.11 and by taking into account the degenerate mass spectrum of the right handed neutrinos, we obtain the mass matrix of the form:

$$M_N = \begin{pmatrix} M & 0 & 0 \\ 0 & 0 & M \\ 0 & M & 0 \end{pmatrix}. \tag{4.14}$$

Field	l_L	$l^c_{R_1}$	$l^c_{R_2}$	$l^c_{R_3}$	N_i	ϕ	η	χ_T	χ_S	χ
A_4	3	1	$1''$	$1'$	3	1	1	3	3	1
Z_4	i	i	i	i	-1	1	1	-1	i	i

Table 4.1 Fields and their respective transformations under the symmetry group of the model.

Now, in order to transform the mass matrix of RHN to a diagonal one, we go to a different basis with the help of an unitary matrix, U, which is represented by:

$$U = \begin{pmatrix} 0 & 0 & 1 \\ 0 & 1 & 0 \\ 1 & 0 & 0 \end{pmatrix}. \tag{4.15}$$

By this change in basis, we further obtain a change in the Yukawa coupling matrix, which is given by:

$$Y = \begin{pmatrix} -a & -a & 2a+b \\ b-a & 2a & -a \\ 2a & b-a & -a \end{pmatrix}. \tag{4.16}$$

Also, it is seen that the charge lepton mass matrix remains diagonal in this new basis:

$$M_l^{'diag} = U^\dagger . M_l . U = M_l^{diag}. \tag{4.17}$$

As already mentioned, the realisation of scotogenic model is done through $A_4 \times Z_4$ flavor symmetry in this study. Within this model, a loop contribution factor $\mathrm{r_i}$ is adressed via the relation $\mathrm{r_i} \propto \frac{1}{\mathrm{M_{N_i}}}$ [198, 192]. So, the contribution of right handed neutrino can be given by $\mathrm{diag}(\mathrm{r_1}, \mathrm{r_2}, \mathrm{r_3})$. However, due to the degeneracy in the RHN masses, the loop factor also becomes degenerate. Using Eq.4.7, the light neutrino mass matrix arising from the loop diagram Fig.4.1 is of the following from:

$$M_{\nu_l} = \begin{pmatrix} K_1 & K_2 & K_2 \\ K_2 & K_3 & K_4 \\ K_2 & K_4 & K_3 \end{pmatrix} \tag{4.18}$$

Eq.4.18 results in a $\mu-\tau$ symmetric light neutrino mass matrix. Therefore, we concentrate on generation of realistic neutrino mixing i.e. non zero θ_{13}, which requires deviation from exact $\mu-\tau$ symmetric mass matrix. To break the $\mu-\tau$ symmetry we have to consider the non-degenerate right handed neutrino mass spectrum. Firstly we will take the condition $r_1 \neq r_2 = r_3 = r$ and further split the degeneracy of N_2 and N_3 by a small amount d, i.e $r_3 = r_2 + d$. Now the structure of the light neutrino mass matrix given in Eq (4.18) will deviate by say M^0 which is proportional to d. So the elements of light neutrino mass matrix(M) after considering $r_1 \neq r_2 = r_3 = r$ are given as follows:

$$m_{11} = \frac{\pi^2}{16}\Bigg[a^2 r_1\Bigg\{\frac{-P\log(r_1^2P)}{r_1^2P-1}+\frac{Q\log(r_1^2Q)}{r_1^2Q-1}\Bigg\}+a^2 r\Bigg\{\frac{-P\log(r^2P)}{r^2P-1}+\frac{Q\log(r^2Q)}{r^2Q-1}\Bigg\} +(2a+b)^2 r\Bigg\{\frac{-P\log(r^2P)}{r^2P-1}+\frac{Q\log(r^2Q)}{r^2Q-1}\Bigg\}\Bigg] \tag{4.19}$$

$$m_{12} = a\frac{\pi^2}{16}\Bigg[-(-a+b)r_1\Bigg\{\frac{-P\log(r1^2P)}{r_1^2P-1}+\frac{Q\log(r_1^2Q)}{r_1^2Q-1}\Bigg\}-2ar\Bigg\{\frac{-P\log(r^2P)}{r^2P-1}+\frac{Q\log(r^2Q)}{r^2Q-1}\Bigg\} -(2a+b)r\Bigg\{\frac{-P\log(r^2P)}{r^2P-1}+\frac{Q\log(r^2Q)}{r^2Q-1}\Bigg\}\Bigg] \tag{4.20}$$

$$m_{13} = a\frac{\pi^2}{16}\Bigg[-2ar_1\Bigg\{\frac{-P\log(r_1^2P)}{r_1^2P-1}+\frac{Q\log(r_1^2Q)}{r_1^2Q-1}\Bigg\}-(-a-b)r\Bigg\{\frac{-P\log(r^2P)}{r^2P-1}+\frac{Q\log(r^2Q)}{r^2Q-1}\Bigg\} -(2a+b)r\Bigg\{\frac{-P\log(r^2P)}{r^2P-1}+\frac{Q\log(r^2Q)}{r^2Q-1}\Bigg\}\Bigg] \tag{4.21}$$

$$m_{22} = \frac{\pi^2}{16}\Bigg[(a-b)^2 r_1\Bigg\{\frac{-P\log(r_1^2P)}{r_1^2P-1}+\frac{Q\log(r_1^2Q)}{r_1^2Q-1}\Bigg\}+4a^2 r\Bigg\{\frac{-P\log(r^2P)}{r^2P-1}+\frac{Q\log(r^2Q)}{r^2Q-1}\Bigg\} +a^2 r\Bigg\{\frac{-P\log(r^2P)}{r^2P-1}+\frac{Q\log(r^2Q)}{r^2Q-1}\Bigg\}\Bigg] \tag{4.22}$$

$$m_{23} = a\frac{\pi^2}{16}\left[2(-a+b)r_1\left\{\frac{-P\log(r_1^2P)}{r_1^2P-1}+\frac{Q\log(r_1^2Q)}{r_1^2Q-1}\right\}+2(-a+b)r\left\{\frac{-P\log(r^2P)}{r^2P-1}+\frac{Q\log(r^2Q)}{r^2Q-1}\right\}\right.$$
$$\left.+ar\left\{\frac{-P\log(r^2P)}{r^2P-1}+\frac{Q\log(r^2Q)}{r^2Q-1}\right\}\right] \tag{4.23}$$

$$m_{33} = \frac{\pi^2}{16}\left[4a^2r_1\left\{\frac{-P\log(r_1^2P)}{r_1^2P-1}+\frac{Q\log(r_1^2Q)}{r_1^2Q-1}\right\}+(a-b)^2r\left\{\frac{-P\log(r^2P)}{r^2P-1}+\frac{Q\log(r^2Q)}{r^2Q-1}\right\}\right.$$
$$\left.+a^2r\left\{\frac{-P\log(r^2P)}{r^2P-1}+\frac{Q\log(r^2Q)}{r^2Q-1}\right\}\right] \tag{4.24}$$

where, $P = m^2 + v^2(\lambda_3+\lambda_4-\lambda_5)$ and $Q = m^2 + v^2(\lambda_3+\lambda_4+\lambda_5)$ with v signifying the vev of the SM Higgs and λ_2, λ_3, λ_4, λ_5 are the quartic couplings.

Now the final light neutrino mass matrix after splitting the degereracy of N_2 and N_3 with a small perturbation d can be written as:

$$M_{\nu_l} = M + M^0 \tag{4.25}$$

where,

$$M^0 = d\begin{pmatrix} 0 & 0 & x \\ 0 & x & 0 \\ x & 0 & 0 \end{pmatrix} \tag{4.26}$$

with $x = 2\lambda_5 v^2$.

4.4 Lepton flavor violating processes :

No experiment so far has observed a flavor violating process involving charged leptons. However, many experiments are currently going on to set strong limits on the most relevant LFV observables, in order to constraint parameter space involved in many new physics models. In this section we will discuss various lepton flavor violating processes (LFV) such

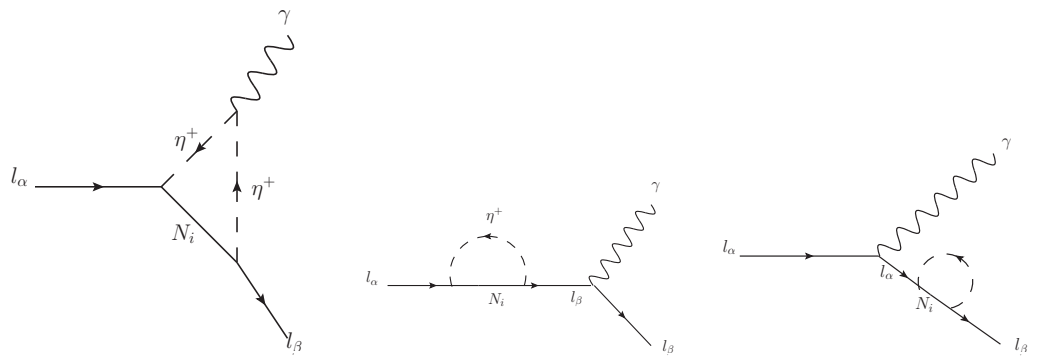

Fig. 4.3 The 1-loop Feynman diagrams giving rise to $l_\alpha \longrightarrow l_\beta \gamma$.

as $l_\alpha \to l_\beta \gamma$,$l_\alpha \to 3l_\beta$ and $\mu - e$ conversion in nuclei [199, 200]. Currently muon decay experiments are most prominent in nature which provides stringent limits for most models. The MEG collaboration [41] has been able to set the impressive bound on muon decay $\mathrm{BR}(\mathrm{l}_\alpha \to \mathrm{l}_\beta \gamma) < 4.2 \times 10^{-13}$. This is expected to improve as the experiment is upgraded to MEG II. In case of $l_\alpha \to 3l_\beta$ decay, contraints comes from SINDRUM experiment [42] to be $\mathrm{BR}(\mathrm{l}_\alpha \to 3\mathrm{l}_\beta) < 10^{-12}$ which is set long ago. The future Mu3e experiment announces a sensitivity of 10^{-16}, which would imply a 4 orders of magnitude improvement on the current bound.

The neutrinoless $\mu - e$ conversion of muonic atom is the most interseting developments regarding the LFV processes [119]. There are many experiments which will basically aim for the positive signal. DeeMe [120], Mu2e [121], COMET [122] and PRIME [123] are such experiments primarily focusing on $\mu - e$ conversion of muonic atom. The sensitivity of these experiments will range from 10^{-14} to 10^{-18}. The current limits on τ observables are less stringent, but will also get improved in the near future by the LHC collaboration , as well as by B-factories such as Belle II [124]. In this part we will discuss the analytical results of branching ratios of different LFV processes such as $l_\alpha \to l_\beta \gamma$,$l_\alpha \to 3l_\beta$ and $\mu - e$ conversion in nuclei within the framework of scotogenic model.

In case of radiative lepton decay, the branching ratio of $l_\alpha \to l_\beta \gamma$ is given by[187]-

$$\mathrm{BR}(\mathrm{l}_\alpha \to \mathrm{l}_\beta \gamma) = \frac{3(4\pi^3)\alpha_{\mathrm{em}}}{4\mathrm{G}_\mathrm{F}^2}|\mathrm{A_D}|^2 \mathrm{BR}(\mathrm{l}_\alpha \to \mathrm{l}_\beta \nu_\alpha \bar{\nu\beta}). \tag{4.27}$$

Here, $\mathrm{G_F}$ is the Fermi constant and $\alpha_{\mathrm{em}} = \frac{\mathrm{e}^2}{4\pi}$ is the electromagnetic fine structure constant, with e the electromagnetic coupling. $\mathrm{A_D}$ is the dipole form factor which is given by-

$$A_D = \sum_{i=1}^{3} \frac{Y^*_{i\beta} Y_{i\alpha}}{2(4\pi)^2} \frac{1}{m^2_{\eta^+}} F_2(\rho_i) \tag{4.28}$$

where the parameter ρ_i is defined as $\rho_i = \frac{M^2_{N_i}}{m^2_{\eta^+}}$ and the loop function $F_2(x)$ is given in appendix.

For three body decay process like $l_\alpha \to 3l_\beta$, the branching ratio is given by-

$$\begin{aligned}\mathrm{BR}(\mathrm{l}_\alpha \to 3\mathrm{l}_\beta) = \frac{3(4\pi^2)\alpha^2_{\mathrm{em}}}{8\mathrm{G}_\mathrm{F}^2} \Bigg[|\mathrm{A_{ND}}|^2 + |\mathrm{A_D}|^2 \left(\frac{16}{3} \log\left(\frac{\mathrm{m}_\alpha}{\mathrm{m}_\beta}\right) - \frac{22}{3} \right) \\ + \frac{1}{6}|\mathrm{B}|^2 + \left(-2\mathrm{A_{ND}}\mathrm{A_D^*} + \frac{1}{3}\mathrm{A_{ND}}\mathrm{B}^* - \frac{2}{3}\mathrm{A_D}\mathrm{B}^* + \mathrm{h.c} \right) \Bigg] \\ \times \mathrm{BR}(\mathrm{l}_\alpha \to \mathrm{l}_\beta \nu_\alpha \bar{\nu\beta}).\end{aligned} \tag{4.29}$$

Here, we have kept $m_\beta << m_\alpha$ only in the logarithmic term, where it avoids the appearance of an infrared divergence. The form factor A_D is generated by dipole photon penguins and is given in equation 17. Regarding the other form factors A_{ND} is given by-

$$A_{ND} = \sum_{i=1}^{3} \frac{Y^*_{i\beta} Y_{i\alpha}}{6(4\pi)^2} \frac{1}{m^2_{\eta^+}} G_2(\rho_i). \tag{4.30}$$

$\mathrm{A_{ND}}$ is generated by non-dipole photon penguins, whereas B, induced by box diagrams is given by-

$$\mathrm{e}^2\mathrm{B} = \frac{1}{(4\pi)^2 \mathrm{m}^2_{\eta^+}} \sum_{\mathrm{i,j}=1}^{3} \left[\frac{1}{2}\mathrm{D}_1(\rho_\mathrm{i}, \rho_\mathrm{j}) \mathrm{Y}^*_{\mathrm{j}\beta} \mathrm{Y}_{\mathrm{j}\beta} \mathrm{Y}^*_{\mathrm{i}\beta} \mathrm{Y}_{\mathrm{i}\alpha} + \sqrt{\rho_\mathrm{i}\rho_\mathrm{j}} \mathrm{D}_2(\rho_\mathrm{i}, \rho_\mathrm{j}) \mathrm{Y}^*_{\mathrm{j}\beta} \mathrm{Y}^*_{\mathrm{j}\beta} \mathrm{Y}_{\mathrm{i}\beta} \mathrm{Y}_{\mathrm{i}\alpha} \right]. \tag{4.31}$$

The loop functions $\mathrm{G}_2(\mathrm{x})$, $\mathrm{D}_1(\mathrm{x},\mathrm{y})$ and $\mathrm{D}_2(\mathrm{x},\mathrm{y})$ are defined in appendix. Here, e Z-boson penguin contributions are negligible, since in this model they are suppressed by charged

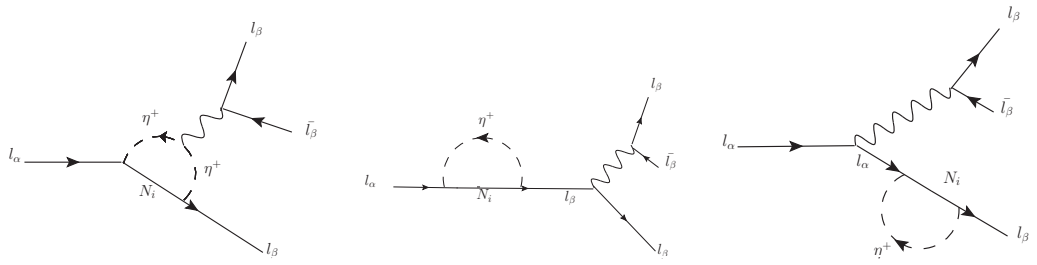

Fig. 4.4 The penguin contributions to $l_\alpha \longrightarrow l_\beta \gamma$, where the wavy lines depicts either a Z-boson or a photon.

lepton masses. Similarly, Higgs-penguin contribution is also supressed which are not taken into consideration. Next we consider the case of $\mu - e$ conversion in nuclei. The conversion rate, normalized to the muon capture rate, can be expressed as -

$$\mathrm{CR}(\mu - \mathrm{e}, \mathrm{Nucleus}) = \frac{\mathrm{p_e E_e m_\mu^3 G_F^2 \alpha_{em}^3 Z_{eff}^4 F_p^2}}{8\pi^2 \mathrm{Z}\Gamma_{\mathrm{capt}}} \times \Big[|(\mathrm{Z}+\mathrm{N})(\mathrm{g}_{\mathrm{LV}}^{(0)} + \mathrm{g}_{\mathrm{LS}}^{(0)}) + (\mathrm{Z}-\mathrm{N})(\mathrm{g}_{\mathrm{LV}}^{(1)} + \mathrm{g}_{\mathrm{LS}}^{(1)})|^2 + |(\mathrm{Z}+\mathrm{N})(\mathrm{g}_{\mathrm{RV}}^{(0)} + \mathrm{g}_{\mathrm{RS}}^{(0)}) + (\mathrm{Z}-\mathrm{N})(\mathrm{g}_{\mathrm{RV}}^{(1)} + \mathrm{g}_{\mathrm{RS}}^{(1)})|^2 \Big] \tag{4.32}$$

here, number of photon and neutron is given by Z and N. $\mathrm{Z_{eff}}$ is the effective atomic charge, F_p denotes the nuclear matrix element and total muon capture rate is denoted by Γ_{capt}. The values of these parameter are different for different nucleus under consideration. Also, $\mathrm{p_e}$ and E_e are the momentum and energy of electron. The expression for $g_{XK}^{(0)}$ and $g_{XK}^{(1)}$ (X=L,R and K=S,V) present in the above equation is given by-

$$g_{XK}^{(0)} = \frac{1}{2} \sum_{q=u,d,s} \left(g_{XK}(q) G_K^{q,p} + g_{XK}(q) G_K^{q,n} \right) \tag{4.33}$$

$$g_{XK}^{(1)} = \frac{1}{2} \sum_{q=u,d,s} \left(g_{XK}(q) G_K^{q,p} - g_{XK}(q) G_K^{q,n} \right). \tag{4.34}$$

Numerical values of G_K are given in various literatures. Again the effective couplings $g_{XK}(q)$ in scotogenic model has many contributions, which are given below-

$$g_{LV}(q) \approx g_{LV}^{\gamma}(q) \tag{4.35}$$

$$g_{RV}(q) = g_{LV}(q)|_{L\leftrightarrow R} \tag{4.36}$$

$$g_{LS}(q) \approx 0 \tag{4.37}$$

$$g_{RS}(q) \approx 0 \tag{4.38}$$

where $g^{\gamma}_{LV}(q)$ stands for the contribution due to photon penguins. Because of the inbuilt Z_2 symmetry in scotogenic model, there is no box contribution to $\mu - e$ conversion of nuclei. This additional symmetry forbids the coupling between scalars(η^+ and η^-) and the quark sector. Regarding the Z-boson penguins contributions, they turn out to be suppressed by charged lepton masses. So the effective coupling can be written as-

$$g^{\gamma}_{LV}(q) = \frac{\sqrt{2}}{G_F} e^2 Q_p (A_{ND} - A_D). \tag{4.39}$$

The form factors A_{ND} and A_D have been already defined. Furthermore, Q_p is the electric charge of the corresponding quark.

4.5 Leptogenesis

We study baryogenesis in the Scotogenic model realised by $A_4 \times Z_4$ symmetry. We can produce observed baryogenesis via the mechanism of leptogenesis [179] in our model. However, the leptogenesis process must occur by the out of equilibrium decay of the RHN, in our case N_1. As discussed in many literatures [189, 190], we now know that there exists a lower bound of about 10TeV for the lightest of the RHNs(M_{N_1}) in the Scotogenic model considering the vanilla leptogenesis scenario [180, 110]. For a heirarchical mass of RHN, i.e $M_{N_1} << M_{N_2}, M_{N_3}$, the leptogenesis produced by the decay of N_2 and N_3 are supressed due to the strong washout effects produced by N_1 or N_2 and N_3 mediated interactions [110]. Thereby, the lepton asymmetry is produced only by the virtue of N_1 decay and this is further converted into the baryon asymmetry of the Universe(BAU) by the electro-weak sphaleron phase transitions [111]. Now for the generation of BAU, we solve the simultaneous

Boltzmann equations for N_1 decay and formation of N_{B-L}. The B-L calculation depends on the comparison between the decay rates for $N_1 \to l\eta, \bar{l}\eta^*$ processes and the Hubble parameter, which causes a certain impact on the asymmetry as well as on the CP-asymmetry parameter ε_1. In the calculation of leptogenesis, one important quantity that differentiates between weak and strong washout regime is the decay parameter. It is expressed as:

$$K_1 = \frac{\Gamma_1}{H(z=1)}, \tag{4.40}$$

where, Γ_2 gives us the total N_2 decay width, H is the Hubble parameter and $z = \frac{M_{N_1}}{T}$ with T being the temperature of the photon bath. We can express H in terms of T and the corresponding equation is given by:

$$H = \sqrt{\frac{8\pi^3 g_*}{90}} \frac{T^2}{M_{Pl}}. \tag{4.41}$$

In Eq.(4.41), g_* stands for the effective number of relativistic degrees of freedom and $M_{Pl} \simeq 1.22 \times 10^{19}$ GeV is the Planck mass. We have introduced a perturbation (ξ) in our work to generate non-zero θ_{13} by breaking the $\mu - \tau$ symmetry. Thus we obtain a non-degeneracy in the RHN masses as discussed in the above section4.3. The mass of the lightest RHN is fixed in the range $M_{N_1} = 10^4 - 10^5$ GeV and that of N_2 is $M_{N_2} = 10^8 - 10^9$ GeV. The range of M_{N_3} will be evaluated considering the relation $M_{N_3} = M_{N_2} + d$. Now, by this choice of RHN masses along with $m_{\eta_R^0} = 400 - 800$ GeV and most significantly the lightest active neutrino mass $m_1 = 10^{-13} - 10^{-12}$ eV, we fall on the weak washout regime. The Yukawa couplings obtained by solving the model parameters are incorporated in the decay rate equation for N_1 which is given by,

$$\Gamma_1 = \frac{M_{N_1}}{8\pi}(Y^\dagger Y)_{11}\left[1 - \left(\frac{m_{\eta_R^0}}{M_{N_1}}\right)^2\right]^2 = \frac{M_{N_1}}{8\pi}(Y^\dagger Y)_{11}(1-\eta_1)^2 \tag{4.42}$$

Again for the decays $N_1 \to l\eta, \bar{l}\eta^*$, the CP asymmetry parameter ε_1 is given by,

$$\varepsilon_1 = \frac{1}{8\pi(Y^\dagger Y)_{11}} \sum_{j\neq 1} Im[(Y^\dagger Y)^2]_{1j} \left[f(r_{j1}, \eta_1) - \frac{\sqrt{r_{j1}}}{r_{j1}-1}(1-\eta_1)^2 \right], \tag{4.43}$$

where,

$$f(r_{j1}, \eta_1) = \sqrt{r_{j1}} \left[1 + \frac{(1-2\eta_1 + r_{j1})}{(1-\eta_1)^2} ln(\frac{r_{j1} - \eta_1^2}{1-2\eta_1 + r_{j1}}) \right], \tag{4.44}$$

and $r_{j1} = (\frac{M_{N_j}}{M_{N_1}})^2$, $\eta_1 \equiv (\frac{m_{\eta_R^0}}{M_{N_1}})^2$.

The Boltzmann equations for the number densities of N_1 and N_{B-L}, given by [189],

$$\frac{dn_{N_1}}{dz} = -D_1(n_{N_1} - n_{N_1}^{eq}), \tag{4.45}$$

$$\frac{dn_{B-L}}{dz} = -\varepsilon_1 D_1(n_{N_1} - n_{N_1}^{eq}) - W_1 n_{B-L}, \tag{4.46}$$

respectively. $n_{N_1}^{eq} = \frac{z^2}{2}K_1(z)$ is the equilibrium number density of N_1, where $K_i(z)$ is the modified Bessel function of i^{th} type and

$$D_1 \equiv \frac{\Gamma_1}{Hz} = K_{N_1} z \frac{K_1(z)}{K_2(z)} \tag{4.47}$$

gives the measure of the total decay rate with respect to the Hubble rate, and $W_1 = \frac{\Gamma_W}{Hz}$ is the total washout rate. Again, $W_1 = W_{1D} + W_{\Delta L=2}$, i.e the total washout term is the sum of the washout due to inverse decays $l\eta, \bar{l}\eta^* \to N_1$ ($W_{1D} = \frac{1}{4}K_{N_1} z^3 K_1(z)$) and the washout due to the $\Delta L = 2$ scatterings $l\eta \leftrightarrow \bar{l}\eta^*, ll \leftrightarrow \eta^*\eta^*$ which is given by,

$$W_{\Delta L=2} \simeq \frac{18\sqrt{10}M_{Pl}}{\pi^4 g_l \sqrt{g_*} z^2 v^4} (\frac{2\pi^2}{\lambda_5})^2 M_{N_1} \bar{m_\varsigma}^2. \tag{4.48}$$

Here, g_l is the internal degrees of freedom for the SM leptons, and $\bar{m_\varsigma}$ is the effective neutrino mass parameter, defined by:

$$\bar{m_\varsigma}^2 \simeq 4\varsigma_1^2 m_1^2 + \varsigma_2 m^{2_2} + \varsigma_3^2 m_3^2, \tag{4.49}$$

where $m_i's$ is the light neutrino mass eigenvalues and ς_k is as defined as:

$$\varsigma_k = \left(\frac{M_{N_k}^2}{8(m_{\eta_R^0}^2 - m_{\eta_I^0}^2)}[L_k(m_{\eta_R^0}^2) - L_k(m_{\eta_I^0}^2)]\right)^{-1} \tag{4.50}$$

The final B-L asymmetry n_{B-L}^f is evaluated by numerically calculating Eq.(4.45) and Eq.(4.46) before the sphaleron freeze-out. This is converted into the baryon-to-photon ratio given by:

$$n_B = \frac{3}{4}\frac{g_*^0}{g_*} a_{sph} n_{B-L}^f \simeq 9.2 \times 10^{-3} n_{B-L}^f, \tag{4.51}$$

In Eq.(4.51), $g_* = 110.75$ is the effective relativistic degrees of freedom at the time when final lepton asymmetry was produced, $g_*^0 = \frac{43}{11}$ is the effective degrees of freedom at the recombination epoch and $a_{sph} = \frac{8}{23}$ is the sphaleron conversion factor taking two Higgs doublet into consideration. The Planck limit 2018 gives a bound on the observed BAU(n_B^{obs}) to be $(6.04 \pm 0.08) \times 10^{-10}$[201]. Therefore, in our work we have chosen the free parameters appropriately so as to generate the observed BAU. The values of the quartic coupling, λ_5 is taken in range $10^{-8} - 10^{-4}$ for successful generation of leptogenesis as well as to have significant results for LFV.

4.6 Numerical Analysis

In our work, we do a random scan for the free parameters of our model given by:

$$\mathrm{M_{N_1}}, \mathrm{M_{N_2}}, \eta_{\mathrm{R}}^0, \lambda_5 \tag{4.52}$$

The values of the above mentioned parameters for which we study the impact on neutrino mass, LFV and BAU are given in the Table4.2 as follows:

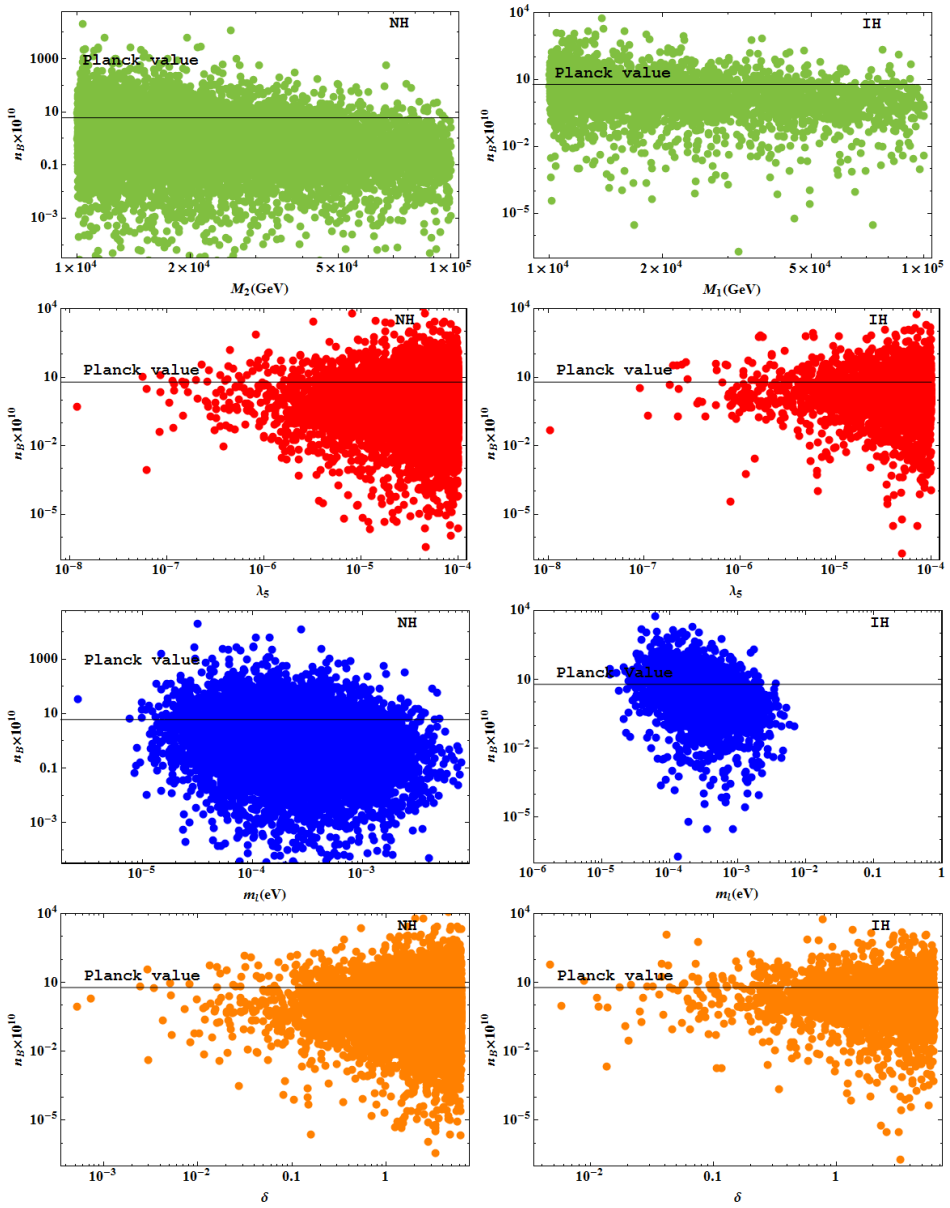

Fig. 4.5 Plots in the first-row shows baryon asymmetry as a function of RHN (M_{N_1}), the second-row shows baryon asymmetry as a function of the quartic coupling (λ_5), in third-row baryon asymmetry as a function of lightest neutrino mass eigenvalue(m_l) is depicted and in the fourth row a variation between leptonic Dirac CP phase(δ) and baryon asymmetry is shown respectively. The black horizontal line gives the current Planck value for BAU.

Parameter	Parameter space
M_{N_1}	10^4 GeV - 10^5 GeV
M_{N_2}	10^8 GeV - 10^9 GeV
η_R^0	400 GeV- 800 GeV
λ_5	10^{-8}- 10^{-4}

Table 4.2 Free parameters of the model and their respective parameter space.

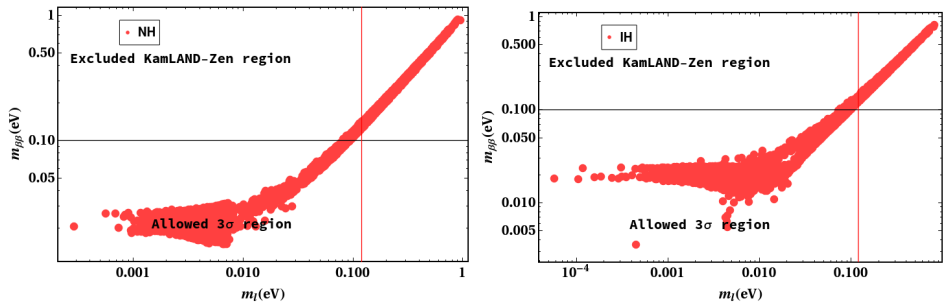

Fig. 4.6 Effective mass as a function of lightest neutrino mass eigenvalue(m_l) for NH/IH. The horizontal(black) line is the upper limit for the effective mass ($m_{\beta\beta}(eV) \sim 0.1(eV)$) of light neutrinos obtained from KamLAND-Zen experiment and the vertical red line depicts the Planck limit for the sum of the light neutrino masses.

We choose the parameter space in such a way so as to fulfill the constraints coming from various phenomenologies. Considering the lightest RHN in TeV scale is a significant characteristic for vanilla leptogenesis in Scotogenic model [180, 202]. A lower bound of about 10 TeV is set for N_1, which has been verified in many literatures [110, 180]. Again, an inert Higgs doublet cannot possibly produce the observed relic density in the mass regime $M_W < M_{DM} \leq 550$ GeV, also called the IHDM desert. Thus, we have considered the lightest of the inert scalar doublet in the range given in Table.(4.2) in order to abide by the bounds from Planck limit to be a probable dark matter candidate and also to check its viability in the range 400-800 GeV. Again the charged scalar(η_+) of the inert doublet is taken to be $(\eta_R^0 + 5)$ GeV, following the constraints from LEP II [203]. The choice of quartic coupling between the SM Higgs and inert doublet $\lambda_5 \neq 0$ is to cause violation of the lepton number.

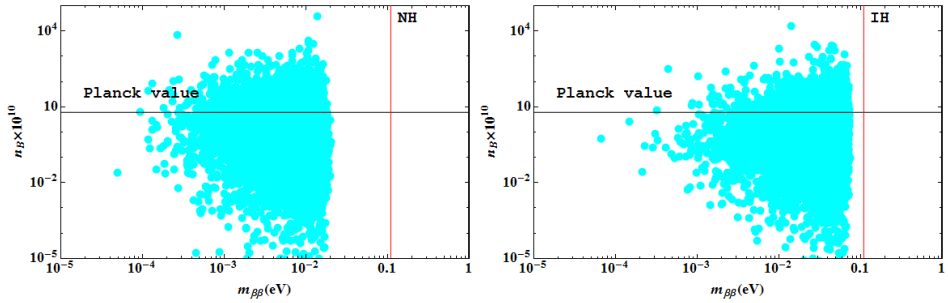

Fig. 4.7 Baryon asymmetry of the Universe as a function of effective mass of active neutrinos($m_{\beta\beta}$) for NH/IH. The horizontal(black) line is Planck value on BAU and the vertical red line depicts the upper bound on the effective mass ($m_{\beta\beta}(eV) \sim 0.1(eV)$) of light neutrinos obtained from KamLAND-Zen experiment.

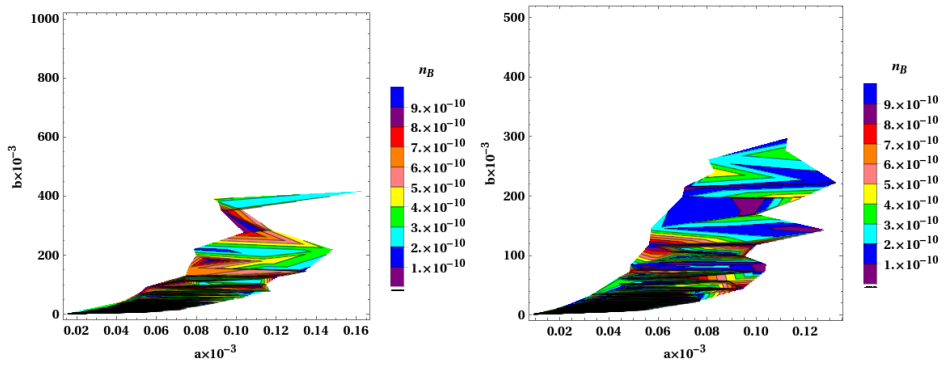

Fig. 4.8 Contour plots relating the model parameter a and b to the baryon asymmetry of the Universe. The left panel is for NH and right panel for IH.

Now, we diagonalise the light neutrino mass matrix ($M_{\nu l}$) by:

$$U_{PMNS}^{T} M_{\nu l} U_{PMNS} = \tilde{M}_{\nu l} = \begin{pmatrix} m_1 & 0 & 0 \\ 0 & m_2 & 0 \\ 0 & 0 & m_3 \end{pmatrix} \tag{4.53}$$

where,

$$U_{PMNS} = \begin{pmatrix} c_{12}c_{13} & s_{12}c_{13} & s_{13}e^{-i\delta} \\ -s_{12}c_{23} - c_{12}s_{23}s_{13}e^{i\delta} & c_{12}c_{23} - s_{12}s_{23}s_{13}e^{i\delta} & s_{23}c_{13} \\ s_{12}s_{23} - c_{12}c_{23}s_{13}e^{i\delta} & -c_{12}s_{23} - s_{12}c_{23}s_{13}e^{i\delta} & c_{23}c_{13} \end{pmatrix} U_{Maj} \tag{4.54}$$

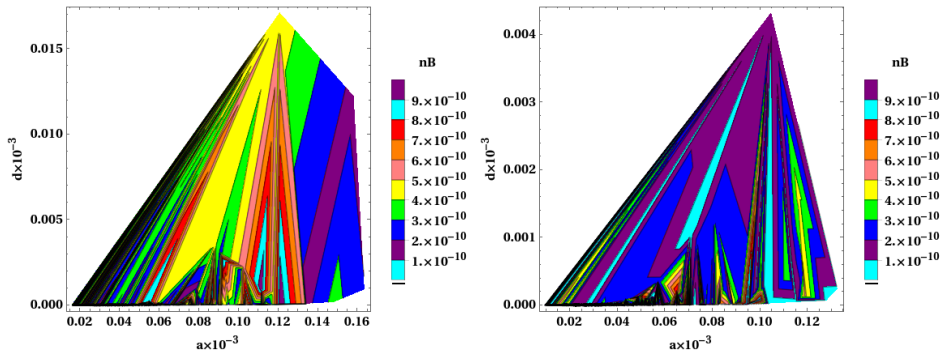

Fig. 4.9 Contour plots relating the model parameter a and d(i.e. the perturbation) to the baryon asymmetry of the Universe. The left panel is for NH and right panel for IH.

is the PMNS (Pontecorvo-Maki-Nakagawa-Sakata) matrix and $c_{ij} = \cos\theta_{ij}$, $s_{ij} = \sin\theta_{ij}$ and δ is the leptonic Dirac CP phase. The diagonal matrix $U_{Maj} = \mathrm{diag}(1, e^{i\alpha}, e^{i(\beta+\delta)})$ contains the Majorana CP phases α, β.

The diagonal mass matrix of the light neutrinos can be written as, $\tilde{M}_{\nu l} = \mathrm{diag}(m_1, \sqrt{m_1^2+\Delta m_{21}^2}, \sqrt{m_1^2+\Delta m}$ for normal hierarchy and $\tilde{M}_{\nu l} = \mathrm{diag}(\sqrt{m_3^2+\Delta m_{23}^2-\Delta m_{21}^2}, \sqrt{m_3^2+\Delta m_{23}^2}, m_3)$ for inverted hierarchy. We then numerical solve the model parameter, thereby generating the light neutrino mass matrix, the Yukawa coupling matrix and the neutrino mixing matrix.

A significant experimental technique of detecting neutrino mass is by the process of neutrinoless double beta decay ($0\nu\beta\beta$) [204–207]. Some of the well known experiments related to it are KamLAND-Zen [208, 209], GERDA [40, 210], KATRIN [211, 212]. We measure the effective neutrino mass $|m_{\beta\beta}|$ expressed by the formula,

$$|m_{\beta\beta}| = \sum_{k=1}^{3} m_k U_{ek}^2 \tag{4.55}$$

where, U_{ek}^2 are the elements of the neutrino mixing matrix with k holding up the generation index. This eq.(4.55) can be further expressed as,

$$|m_{\beta\beta}| = |m_1 U_{ee}^2 + m_2 U_{e\nu}^2 + m_3 U_{e\tau}^2|. \tag{4.56}$$

It is important to check if the model obeys the bound of the effective mass with the lightest neutrino mass so that we can relate the current light neutrino parameters giving correct hints to ongoing experiments and their future sensitivity.

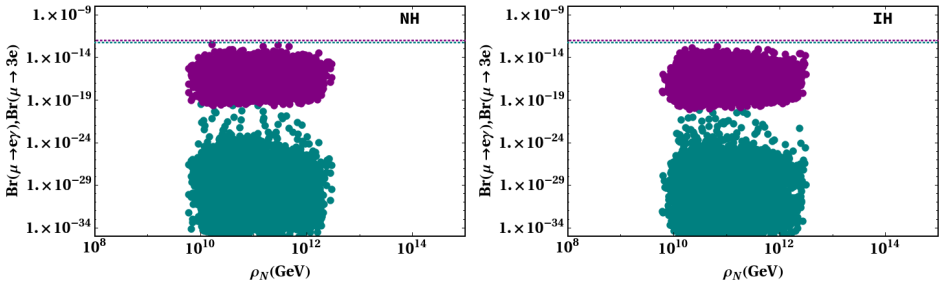

Fig. 4.10 $Br(\mu \to e\gamma)$ and $Br(\mu \to 3e)$ as a function of ρ_N (where $\rho_N = (\frac{M_N}{m_{\eta^+}})^2$) for NH and IH. The dashed horizontal lines are the recent upper bounds

.

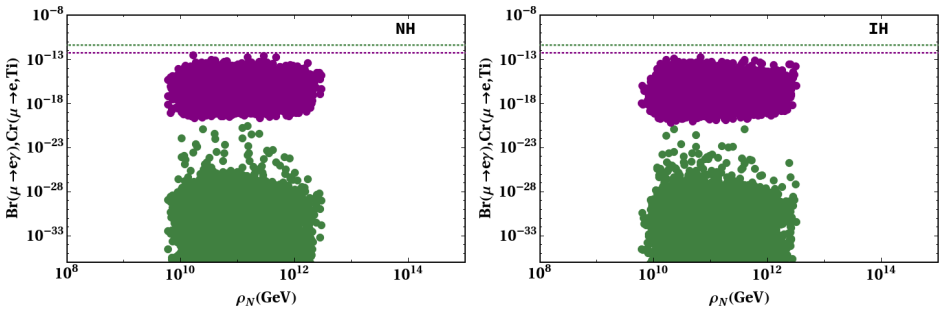

Fig. 4.11 $Br(\mu \to e\gamma)$ and $Cr(\mu \to e, Ti)$ as a function of ρ_N (where $\rho_N = (\frac{M_N}{m_{\eta^+}})^2$) for NH and IH. The dashed horizontal lines are the recent upper bounds.

From Fig.(4.6), we see that the effective mass of the light neutrinos are consistent with the KamLAND-Zen experiment for $m_l = 10^{-4} - 10^{-2}$ eV incase of both NH and IH. A variation between mass of the lightest RHN(M_{N_1}) and BAU for NH/IH is depicted in the first row of Fig.(4.5). We see that the parameter space taken for M_{N_1} is compatible for generating the observed BAU for both NH/IH. The second row of Fig.(4.5) shows that $\lambda_5 = 10^{-6} - 10^{-4}$ has concentrated points satisfying the Planck value for BAU for NH/IH. However, we have fewer points below $\lambda_5 = 10^{-6}$ which satisfy the bound for BAU. Thus, we can conclude that the

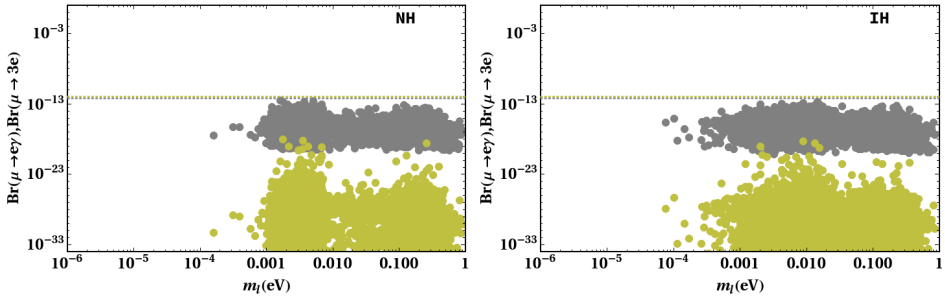

Fig. 4.12 $Br(\mu \to e\gamma)$ and $Br(\mu \to 3e)$ as a function of lightest neutrino mass eigenvalue(m_l) for NH and IH. The dashed horizontal lines are the recent upper bounds.

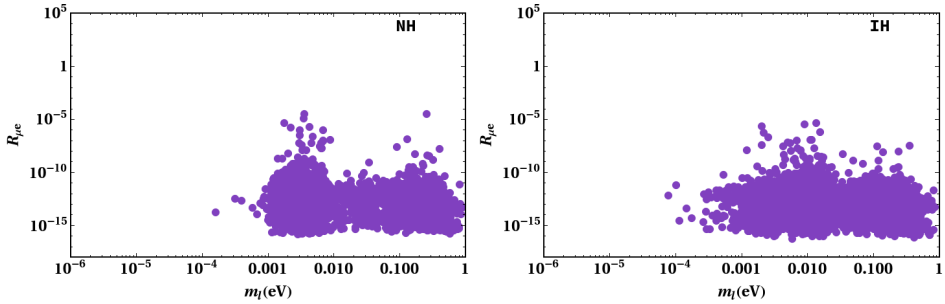

Fig. 4.13 $R_{\mu e}$ as a function of lightest neutrino mass eigenvalue(m_l) for NH and IH. Here, $R_{\mu e} = \frac{Br(\mu \to 3e)}{Br(\mu \to e\gamma)}$.

space $\lambda_5 = 10^{-6} - 10^{-4}$ is consistent with the BAU. Again from the variation plot between the lightest active neutrino mass eigenvalue(m_l) and BAU, we get a constraint region of m_l which satisfies the Planck value for BAU both for NH/IH. Also, interestingly the constraint region of m_l falls within the bounds given by Planck for the summation of the light neutrino masses. The fourth row of Fig.(4.5) shows that the variation of CP violating phase(δ) with the baryon asymmetry of the Universe. Here, we observe that δ value above 10^{-2} satisfies the Planck value for BAU for both NH/IH. A plot of BAU as a function of effective neutrino mass is evaluated as can be seen from Fig.(4.7). It is thereby observed that the effective neutrino mass ranging from $10^{-2} - 10^{-1}$ eV is successful in generating the correct BAU for NH, similar to that incase of IH. In Fig.(4.8), we show a contour plot between the model parameters a and b with the effective mass of light neutrinos. And from Fig.(4.8), we see

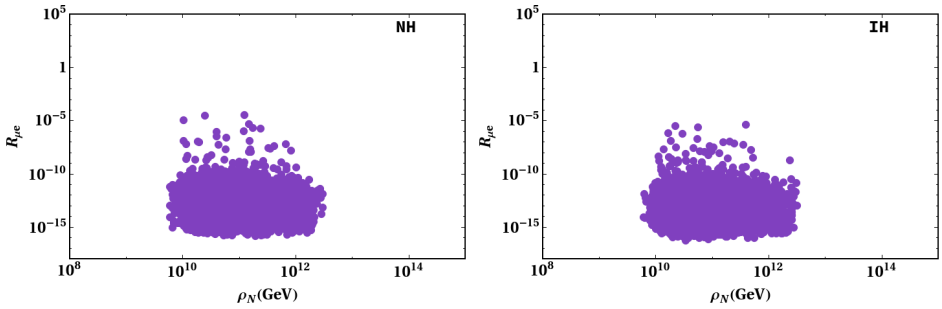

Fig. 4.14 $R_{\mu e}$ as a function of ρ_N for NH and IH. Here, $R_{\mu e} = \frac{Br(\mu \to 3e)}{Br(\mu \to e\gamma)}$.

a co relation between a and b with the baryon asymmetry of the Universe. From these plots, we obtain the range of the model parameters, i.e $a \simeq 0.8 \times 10^{-4} - 0.13 \times 10^{-4}$ and $b \simeq 0.2 - 0.4$ which further gives rise to a constraint in the Yukawa coupling matrix with its elements having values less than 3.We have considered a perturbation d in order to break the degeneracy of the RHN as well as to deviate from the $\mu - \tau$ symmetry. So, in Fig.4.9 we show a contour plot so as to constraint d w.r.t the baryon asymmetry of the Universe.

We have studied the LFV processes within the model. LFV obervables are ploted against different parameters defined within the parameter spaces of the model. Relevant formulae for LFV proceses $l_\alpha \to l_\beta \gamma$, $l_\alpha \to 3l_\beta$ and $\mu - e$ conversion are discussed in section(4.4). We have defined the ratio of branching ratio of two LFV decay $l_\alpha \to l_\beta \gamma$ and $l_\alpha \to 3l_\beta$ as $R_{\mu e}$ [187] i.e

$$\mathrm{R_{\mu e}} = \frac{\mathrm{Br(l_\alpha \to 3l_\beta)}}{\mathrm{Br(l_\alpha \to l_\beta \gamma)}} \tag{4.57}$$

In case of $\mu - e$ conversion the Z-penguins gives a very little contribution compared to γ-penguines. In this sutuation dipole operator will dominate the conversion rate. So, the coversion rate will have a very simple relation given below-

$$\frac{\mathrm{CR}(\mu - \mathrm{e},, \mathrm{Nucleus})}{\mathrm{Br}(\mu \to \mathrm{e}\gamma)} \approx \frac{\mathrm{f(Z,N)}}{428} \tag{4.58}$$

Where $\mathrm{f(Z,N)}$ is a funation which depends on the nucleus and ranges from 1.1 to 2.2 for nuclei of interest i.e titanium.

We have computed all the branching ratio of LFV decays and conversion ratio taking consideration of contraints coming from the model. Variation of $\mathrm{Br}(\mu \to \mathrm{e}\gamma)$ and $\mathrm{Br}(\mu \to 3\mathrm{e})$ as a function of ρ_N (where $\rho_N = (\frac{M_N}{m_{\eta^+}})^2$) is depicted in Fig.(4.10). In this case for both the mass orderings, we get $\mathrm{Br}(\mu \to \mathrm{e}\gamma)$ in the range 10^{-18} to 10^{-13} and $\mathrm{Br}(\mu \to 3\mathrm{e})$ spanning from 10^{-33} to 10^{-23}, which are consistant with current and near future experimental limits. Similarly we have ploted the variation of $\mu - e$ conversion ratio in Fig.(4.11) against ρ_N which is also in the experimental limits. Variation of lightest neutrino mass eigenvalue for both the mass orderings with both the branching ratio $\mathrm{Br}(\mu \to \mathrm{e}\gamma)$ and $\mathrm{Br}(\mu \to 3\mathrm{e})$ is given in Fig.(4.12). From this we can see that for both the mass ordering results are consistant with experimental limit.

In Fig.(4.13) we have ploted the variation of $R_{\mu e}$ which is the ratio of two LFV decays $l_\alpha \to l_\beta \gamma$ and $l_\alpha \to 3l_\beta$ against the lightest neutrino mass eigenvalue for both the mass orderings. From this we can infer that in case of both NH/IH ,$l_\alpha \to l_\beta \gamma$ decay supress the $l_\alpha \to 3l_\beta$ decay in our prameter spaces. Also, we can see that the parameter space of lightest active neutrino mass for which we get this kind of suppression is in the range $10^{-3} - 1\mathrm{eV}$. Further, we have also generated a plot (Fig.(4.14)) depicting the co relation between $R_{\mu e}$ and ρ_N and it is observed that the viable range for ρ_N is $10^{10} - 10^{12}$ GeV. We have shown a common parameter space of the model parameters, satisfying the baryon asymmetry of the Universe in Table 4.3.

Parameter	NH	IH
a	$0.8 \times 10^{-4} - 0.13 \times 10^{-4}$	$0.6 \times 10^{-4} - 0.9 \times 10^{-4}$
b	$0.2 - 0.4$	$0.1 - 0.16$
d	$10^{-6} - 0.15 \times 10^{-4}$	$0.9 \times 10^{-6} - 10^{-6}$

Table 4.3 Model parameters of the model and their respective parameter space satisfying the Planck limit for baryon asymmetry of the Universe.

We see from Table. 4.3 that a larger parameter space of a,b and d are consistent with the Planck limit for BAU incase of NH as compared to that of IH.

4.7 Summary

In this chapter, we have basically realised Ernest Ma's Scotogenic model with the help of discrete symmetries $A_4 \times Z_4$. A $\mu - \tau$ symmetric neutrino mass matrix is obtained, which is thereafter broken by introducing a perturbation to it. This mechanism is required for the generation of realistic neutrino mixing i.e. non zero θ_{13}, deviation of θ_{23} from maximality and small correction in solar mixing angle θ_{12}. As $r_i \propto \frac{1}{M_{N_i}}$, we have broken the degenracy in the masses of the RHN with the implementation of a perturbation which further breaks the $\mu - \tau$ symmetry. We have taken four free parameters, $M_{N_1}, M_{N_2}, \eta_R^0$ and λ_5 whose values are mentioned above. By this choice of the parameter space, we have shown its consistency with various experimental and cosmological bounds. The lightest of the RHN, decays to produce lepton asymmetry which is further converted into BAU. Thus, the parameter space taken into account for the generation of the BAU are seen to follow the Planck value for BAU. From the third row of Fig.(4.5), we can see that the lightest active neutrino mass eigenvalue obtained from the model satisfies the Planck value for BAU and consecutively obeys the Planck limit for the summation of light neutrino masses for NH/IH. Thus, the model is viable in connecting BAU and $0\nu\beta\beta$, also satisfying the bounds coming from neutrino oscillation data. We have also calculated the effective mass of the light neutrinos and shown the results in Fig.(4.6). The lightest active neutrino mass eigenvalue for both NH/IH is seen to satisfy the KamLAND-Zen limit for effective mass of light neutrinos. Additional to this, a contour plot co-relating the model parameters with BAU is also studied. The conclusion we can draw from it is that the parameter space obtained from the model falls within the experimental bounds, thereby constraining the Yukawa coupling matrix. Furthermore, we have computed the branching ratios, $\mathrm{Br}(\mu \to \mathrm{e}\gamma)$ and $\mathrm{Br}(\mu \to 3\mathrm{e})$ of LFV decays along with the $\mu - e$ conversion ratio. A variational plot between the branching ratios and ρ_N is shown in Fig.(4.10), which is conistent with the current and the near future experimental bounds. Also, a similar plot for conversion ratio is also shown in Fig.(4.11), which also satisfies the current

upper bound. We have also studied a co-relation plot between the branching ratios and the lightest neutrino mass eigenvalue and see that it also obeys the experimental upper bounds for the branching ratios. It is predicted well from Fig.(4.13) and Fig.(4.14) that $l_\alpha \to l_\beta \gamma$ decay supress the $l_\alpha \to 3l_\beta$ decay incase of both NH/IH. We can say that the results hardly show any change depending on the mass hierarchies. Overall, this realisation of the Scotogenic model by discrete symmetries, with the considerations on the free parameters taken from various bounds is viable for studying neutrino as well as cosmological phenomenologies.